



Babeş-Bolyai University
Faculty of Chemistry and Chemical Engineering



Ph.D. Thesis Summary

Design, synthesis, and optical properties of new phenothiazinium cationic dyes

Ph.D. Student

Bianca-Alexandra Stoean (married Vasile)

Scientific advisor:

Prof. Dr. Habil. Radu-Lucian Silaghi-Dumitrescu

Cluj-Napoca

2024

Keywords: phenothiazinium dyes, folic acid, ultrasound-assisted synthesis, mechanochemical synthesis, optical properties, fluorophore, photosensitizer, colorimetric oxygen indicator.

CONTENTS

1.	INTRODUCTION.....	4
2.	LITERATURE REVIEW AND STATE OF THE ART.....	9
2.1.	Methylene Blue – the parent compound of the phenothiazin-5-ium dyes class.....	9
2.2.	Synthesis methods and strategies for phenothiazin-5-ium dyes.....	10
2.3.	Optical properties and applications of Methylene Blue and its analogues.....	12
2.4.	Photodynamic therapy and the phenothiazinium dyes as photosensitizers.....	16
3.	ORIGINAL CONTRIBUTIONS.....	19
3.1.	Synthesis and structural characterization of novel phenothiazinium dyes.....	19
3.1.1.	Synthesis of novel phenothiazinium dyes.....	19
3.1.2.	Structural characterization.....	23
3.2.	The impact of auxochrome units on optical and physical properties.....	31
3.2.1.	UV-vis absorption properties.....	32
3.2.2.	Fluorescence emission properties.....	33
3.2.3.	Solvatochromism of the phenothiazinium dyes.....	34
3.2.4.	Aggregation study.....	34
3.3.	Biological activity of the new phenothiazinium dyes.....	36
3.3.1.	Potential theragnostic agents: fluorescence imaging and antitumoral activity evaluation in human ovarian cancer cells.....	36
3.3.2.	New photosensitizers for anticancer photodynamic therapy: efficacy and oxidative stress evaluation in B16F10 melanoma cells.....	44
3.3.3.	Conclusions.....	52
3.4.	Functionalization of phenothiazinium dyes with folic acid.....	52
3.4.1.	Synthesis and structural characterization of the new derivatives.....	52
3.4.2.	Optical and physical properties of the new folates.....	54
3.4.3.	New photosensitizers for antimicrobial photodynamic therapy: efficacy evaluation on Gram-positive and Gram-negative bacterial strains.....	57
3.4.4.	Conclusions.....	63

3.5.	Transient radical species of phenothiazinium dyes and oxygen indicators.....	64
3.5.1.	UV-vis experiments documentation of transient radical species.....	65
3.5.2.	Electron paramagnetic resonance experiments.....	67
3.5.3.	Oxygen colorimetric indicators.....	69
3.5.4.	Conclusions.....	71
4.	MATERIALS AND METHODS.....	73
4.1.	Synthesis and structural characterization.....	73
4.1.1.	General procedure for the synthesis of MB analogues.....	73
4.1.2.	General procedure for the synthesis of folic acid esters FAE 2-4.....	76
4.1.3.	Single crystal X-ray diffraction analysis.....	78
4.2.	Optical and physical properties.....	78
4.2.1.	Fluorescence quantum yield.....	78
4.2.2.	Singlet oxygen photogeneration.....	79
4.2.3.	Lipophilicity assignment using n-octanol/water partition coefficient.....	79
4.3.	Biological activity.....	80
4.3.1.	Cellular fluorescence imaging investigation.....	80
4.3.2.	Biological activity of MBA 2-4 in human ovarian cancer cells.....	81
4.3.3.	Biological activity of MBA 5-7 as photosensitisers in B16-F10 melanoma cells.....	86
4.3.4.	Biological activity of MBA 2-4 and FAE 2-4 as photosensitisers on Gram-positive and Gram-negative bacterial strains.....	88
4.4.	Oxygen colorimetric species.....	89
4.4.1.	UV-vis measurements.....	89
4.4.2.	EPR measurements.....	89
4.4.3.	Chemical oxygen indicators incorporated in carboxymethylcellulose (CMC) polymer matrix ChOxIn.....	90
4.4.4.	Photochemical oxygen indicators containing TiO ₂ -photocatalyst on Polyvinyl alcohol (PVA) support PhOxIn.....	90
4.4.5.	Testing the oxygen indicators.....	90
5.	CONCLUSIONS.....	92
	REFERENCES.....	97
	LIST OF PUBLICATIONS AND CONFERENCE PARTICIPATION.....	114

SUPPORTING INFORMATION.....116

Table of contents of the summary

Introduction.....	6
1. Synthesis and structural characterization of novel phenothiazinium dyes.....	7
1.1. Synthesis of novel phenothiazinium dyes.....	7
1.2. Structural characterization.....	8
2. The impact of auxochrome units on optical and physical properties.....	9
2.1. UV-vis absorption properties.....	10
2.2. Fluorescence emission properties.....	10
2.3. Solvatochromism of the phenothiazinium dyes.....	11
2.4. Aggregation study.....	11
3. Biological activity of the new phenothiazinium dyes.....	12
3.1. Potential theragnostic agents: fluorescence imaging and antitumoral activity evaluation in human ovarian cancer cells.....	12
3.2. New photosensitizers for anticancer photodynamic therapy: efficacy and oxidative stress evaluation in B16F10 melanoma cells.....	13
4. Functionalization of phenothiazinium dyes with folic acid.....	15
4.1. Synthesis and structural characterization of the new derivatives.....	15
4.2. Optical and physical properties of the new folates.....	16
4.3. New photosensitizers for antimicrobial photodynamic therapy: efficacy evaluation on Gram-positive and Gram-negative bacterial strains.....	17
5. Transient radical species of phenothiazinium dyes and oxygen indicators.....	19
5.1. UV-vis experiments documentation of transient radical species.....	19
5.2. Electron paramagnetic resonance experiments.....	20
5.3. Oxygen colorimetric indicators.....	20
6. Conclusions.....	22

Introduction

Of over 5000 compounds based on the phenothiazine scaffold (available in scientific databases) ¹, the majority are represented by methylene blue (MB) analogues ². New strategies for modifying the structures of MB analogues are sought in order to obtain optimized properties such as absorption, fluorescence emission, solubility or lipophilicity, leading to better targeted-therapeutic agents with augmented specificity and diminished side effects ³.

The present thesis focuses on the synthesis and structural characterization of novel phenothiazinium dyes, designed for improved capacity to act as staining agents in fluorescence microscopy for malignant tissues, theragnostic agents or as photosensitizers in photodynamic therapy (anticancer PDT or antimicrobial PDT).

The bio-chemical and physical properties of the synthesised compounds have been enhanced by incorporating various auxochrome units into their design. A comprehensive investigation has been conducted to analyse the effects of the grafted auxochromic units on the UV-vis absorption, fluorescence emission, and solvatochromism of the dyes.

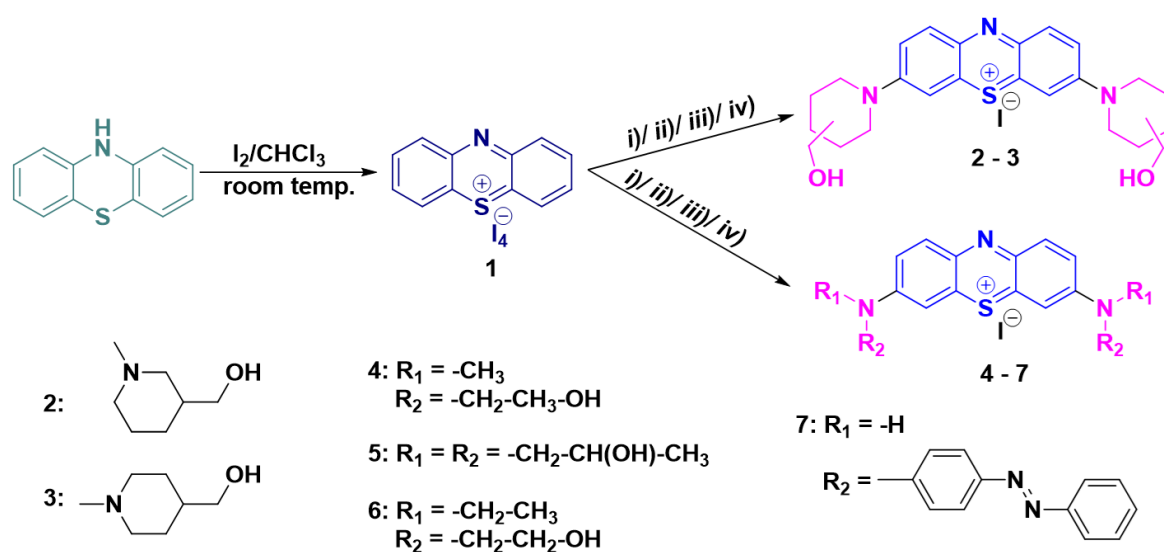
The studies performed for antitumoral activity in human ovarian cancer cells and for effectiveness in PDT against melanoma cells have shown that these phenothiazinium dyes have potential in fluorescence imaging, also as theragnostic agents and photosensitizers, some of them yielding superior outcomes compared to the methylene blue standard. The functionalization of the new MB analogues with folic acid has been investigated in order to improve their targeting ability, particularly for resistant bacteria that are capable of producing folic acid and its derivatives *de novo*.

Three of the synthesised phenothiazinium dyes could also be used as colorimetric oxygen sensors. The radical species of these compounds were also observed and investigated in the studies carried out for this application. Thus, the study of the radical forms helped to better understand the photochemical behaviour and pave the way for other applications both in terms of biomedical and environmental context.

1. Synthesis and structural characterization of novel phenothiazinium dyes

1.1. Synthesis of novel phenothiazinium dyes

To assess the impact of auxochrome groups on the structure-properties relationship of MB analogues, new phenothiazinium dyes were synthesized via nucleophilic substitution of phenothiazinium tetraiodide salt **1** (Scheme 1) with aliphatic or aromatic amines possessing various nucleophilicity characteristics.



Scheme 1. Synthesis of Methylene Blue analogues-MBA **2-7**. Reaction conditions: *i*) ethanol, reflux, 24h; *ii*) mechanical stirring, r.t., 30 min; *iii*) ethanol, indirect ultrasound irradiation, r.t., 45 min; *iv*) ethanol, direct ultrasound irradiation, r.t., 45 min.

To illustrate the variations in biological, physical and chemical properties that can be achieved by grafting various auxochrome groups onto the chromophore scaffold, the following types of nucleophiles have been selected: a) polar, secondary, heterocyclic-aliphatic amines (compounds **MBA 2** and **MBA 3**), b) more polar, secondary-aliphatic amines (compounds **MBA 4-6**) and c) lipophilic, bulky-aromatic-primary amine (compound **MBA 7**).

In addition to the classical (with solvent) method, we reported three new environmentally-friendly methods^{4,5} for synthesizing this type of dyes. These methods include the mechanochemical procedure and the ultrasound irradiation procedures (direct and indirect irradiation), which, with the exception of dye **MBA 7**, yielded superior outcomes (reaction

time, yield and reduced number of purification stapes) in every instance involving the synthesis of compounds **MBA 2-6**.

1.2. Structural characterization

Structural assignments based on high resolution mass spectrometry (HRMS) and nuclear magnetic resonance NMR spectroscopy confirmed the formation of the symmetrical 3,7-disubstituted phenothiazinium salt as the main reaction product. For **MBA 6**, crystals suitable for single crystal X-ray diffraction were obtained and the XRD was recorded.

The analysis of the NMR proton spectra of **MBA 2-7** reveals that the six protons in the phenothiazinium chromophore exhibit three distinct signals in the aromatic region, with chemical shift values ranging from 8.04 ppm to 7.38 ppm. The specific values depend on the substituents grafted in the 3,7 positions. In all cases, the protons H₂ and H₈ gave the most deshielded signals, due to their neighbouring with the withdrawing positivised nitrogen atom (Figure 1).

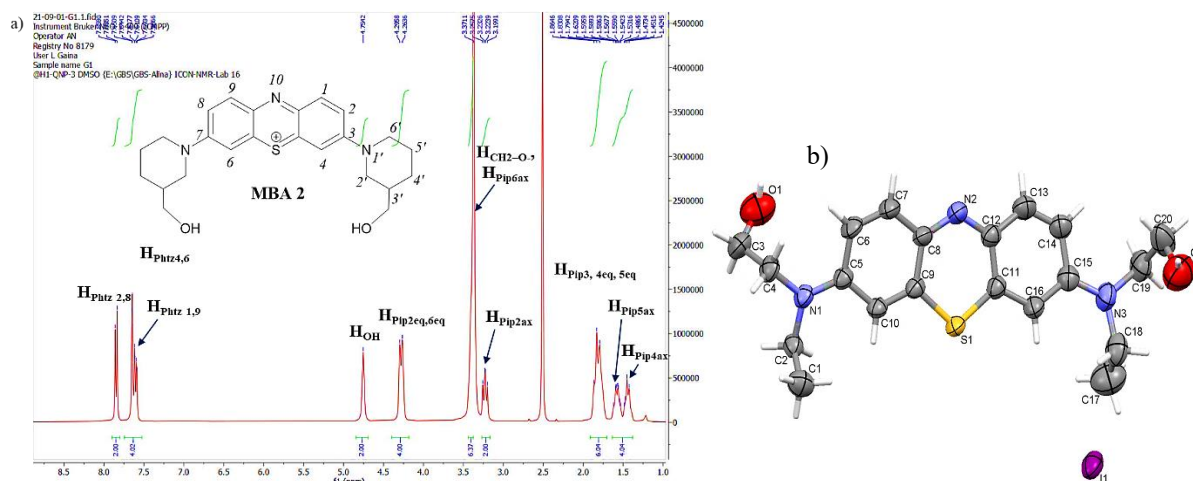
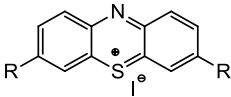
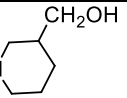
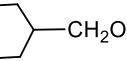
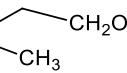
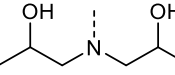
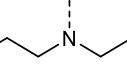
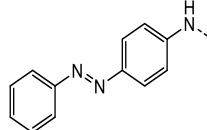


Figure 1. a) ¹H-NMR (400 MHz, DMSO-d₆) spectrum for compound **MBA 2**; b) Asymmetric units of **MBA 6** illustrating the atoms as thermal ellipsoids at 50% probability.

2. The impact of auxochrome units on optical and physical properties

The photophysical properties illustrated by the UV-vis absorption and fluorescence emission spectra of the new phenothiazinium dyes featuring hydrophilic auxochrome units (**MBA 2-6**) and lipophilic 4-phenyldiazenylaniline units (**MBA 7**) as well as those of the parent MB are summarized in Table 1.

Table 1. Photophysical properties of novel phenothiazinium dyes **MBA 2-7**.

	$\lambda_{\max \text{abs}}^a$ [nm]	ϵ [M ⁻¹ cm ⁻¹]	$\lambda_{\max \text{em}}^b$ [nm]	Fluorescence Quantum Yield ϕ_F^c [%]	Stokes shift [cm ⁻¹]	Log P ^d
MB R=--N(CH ₃) ₂	665	7.5x10 ⁴	690	4 ⁶	545	-0.9 ⁷
2 R=---N 	668	5.1x10 ⁴	715	4.6	984	-1.15
3 R=---N 	664	3.9x10 ⁴	698	2.7	734	-1.29
4 R=---N 	660	13.2x10 ⁴	670	11.1	226	-1.21 <-1.6 ⁸
5 R= 	645	25x10 ⁴	691	3.9	1011	-1.96
6 R=HO 	648	30x10 ⁴	685	2.9	834	-1.21
7 R= 	578	5.1x10 ⁴	-	-	-	0.93

^a ethanol solution

^b ethanol solution, $\lambda_{\text{excitation}} = 650$ nm

^c relative to MB standard

^d water/*n*-octanol solution

2.1. UV-vis absorption properties

The visible absorption maxima wavelength for all the **MBA** novel compounds in ethanolic solution are in the 555-668 nm range (Figure 2). Compounds **MBA 2-6** display electronic properties similar to the parent MB. The 4-phenyldiazenylaniline-phenothiazinium iodide **MBA 7** shows much broader absorption bands, with absorption maxima at wavelengths from 555 nm to 668 nm, with no clear dependence on the polarity solvent; self-association and/or complexation with the solvent may explain the differences in this case.

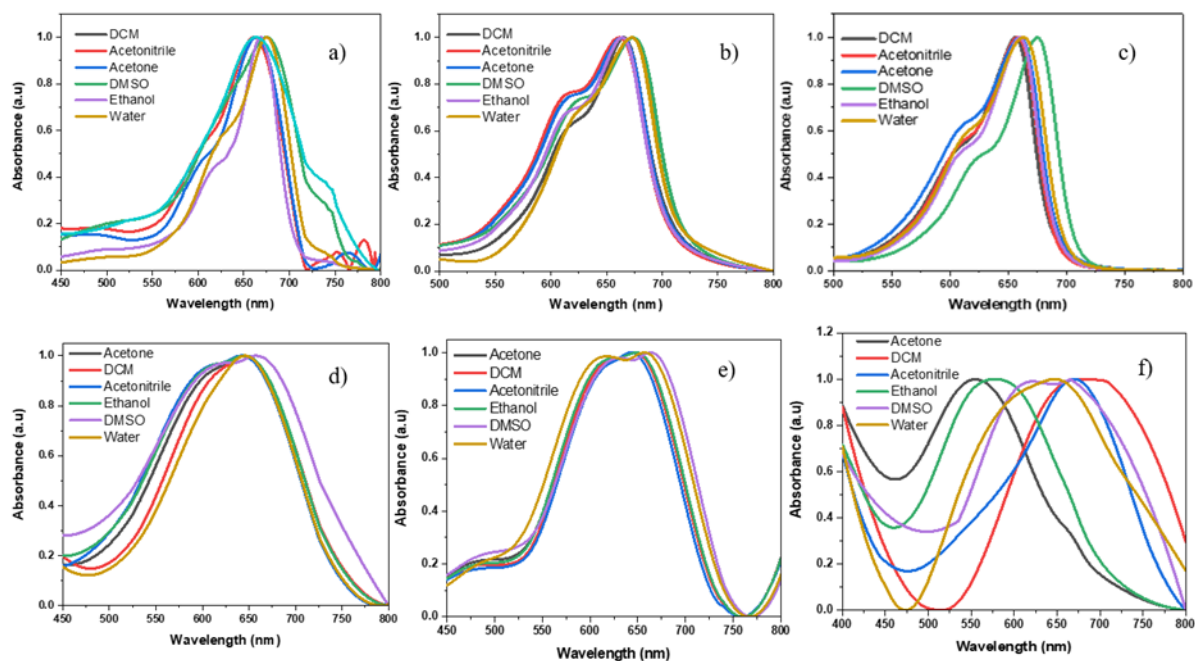


Figure 2. Normalized visible absorption spectra of novel MB analogues at micromolar concentration in solvents of various polarities: a) **MBA 2**; b) **MBA 3**; c) **MBA 4**; d) **MBA 5**; e) **MBA 6**; f) **MBA 7**.

2.2. Fluorescence emission properties

The fluorescence emission spectra of **MBA 2-6** were measured at micromolar concentrations in solvents of various polarities. For **MBA 7**, no fluorescence emission was observed in any solvent. The dyes **MBA 2-6** emitted fluorescence with maximum intensity in the visible range (670-715 nm – Figure 3). The Stokes shift decreased in the sequence $5 > 2 > 6 > 3 > \text{MB} > 4$ (Table 1). **MBA 2** and **MBA 4** gave higher fluorescence quantum yields - 4.6% for **MBA 2** and 11.1% for **MBA 4**, and almost twice Stokes shift (984 cm^{-1} for **MBA 2**) compared to MB (545 cm^{-1}). The highest Stokes shift value (1011 cm^{-1}) was observed for the most hydrophilic dye, **MBA 5**.

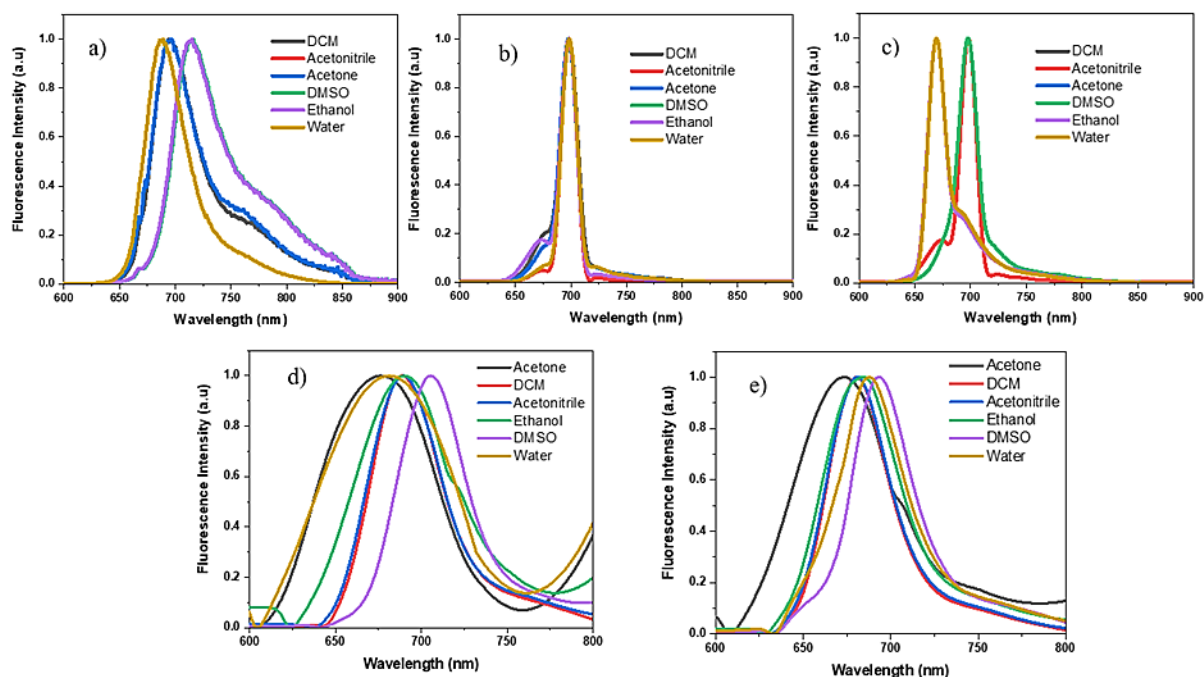


Figure 3. Normalized fluorescence emission spectra of novel phenothiazinium dyes: a) **MBA 2**; b) **MBA 3**; c) **MBA 4**; d) **MBA 5**; e) **MBA 6**, at micromolar concentration in solvents of various polarities.

2.3. Solvatochromism of the phenothiazinium dyes

A red shift of the emission maxima was observed for **MBA 2**, **MBA 4**, **MBA 5** and **MBA 6** in polar, aprotic solvent DMSO, while for **MBA 3** the solvent had no apparent effect. The azo-dye **MBA 7** displays the most pronounced solvatochromism among the new synthesized compounds. The longest absorption wavelength for compound **MBA 7** is obtained in the less polar solvent, dichloromethane ($\lambda_{\text{max,abs}}=680$ nm).

2.4. Aggregation study

An aggregation study of the **MBA 2**, **MBA 3**, **MBA 5** and **MBA 6** performed in aqueous solutions indicated no aggregation tendency within experimental accuracy at micromolar concentration, individual longest wavelength absorption band following the Lambert-Beer law with no evidence of dimerization effects such as a relevant hypsochromic shift or decrease of absorption cross section upon concentration increase at concentrations used in this study. For **MBA 4** a weak dimerization tendency was previously reported⁸. While the absorbance of **MBA 7** decreases with increasing concentration, no additional absorption maximum (typical for dimeric forms) is observed.

3. Biological activity of the new phenothiazinium dyes

3.1. Potential theragnostic agents: fluorescence imaging and antitumoral activity evaluation in human ovarian cancer cells

The cellular uptake of dyes **MBA 2–4** was evaluated aiming their potential for cellular staining of tumoral ovarian cells. As shown in Figure 4, the new **MBA 2, 3** were well internalized by the ovarian cells giving a distinct red fluorescence of the cytoplasm. The intracellular images captured in near infrared domain revealed the best accumulation of dyes **MBA 2–4** in the rich folate-receptor OVCAR-3 cells. **MBA 2** stains both adenocarcinoma cell lines, imparting the brightest red fluorescence to the highly malignant OVCAR-3 cells. **MBA 3** displayed a non-selective affinity for all tested cell types, while **MBA 4** particularly stains the normal BJ cells.

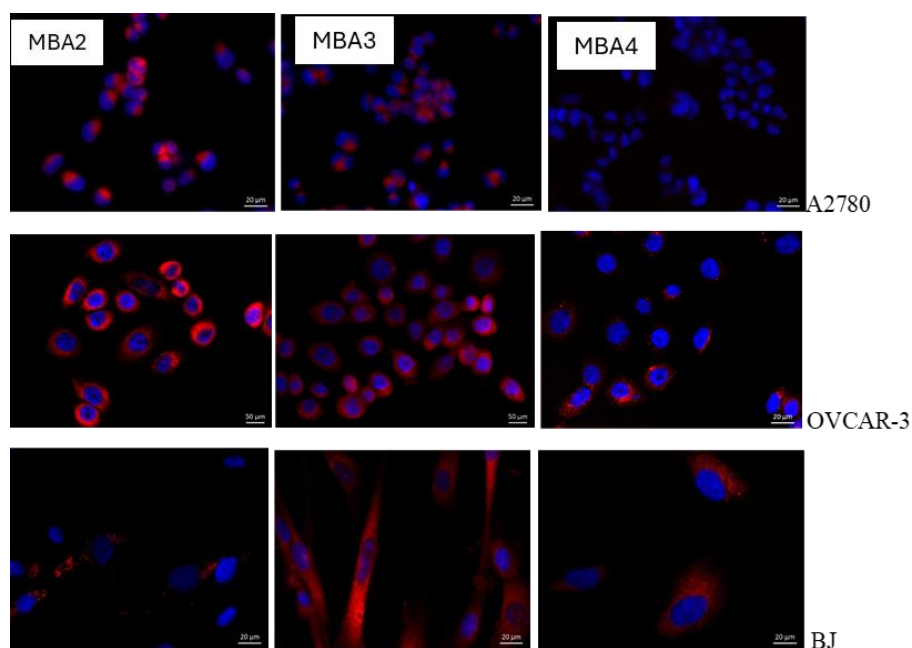


Figure 4. Fluorescence microscopy imaging revealing the *in vitro* cellular uptake of the MB analogues in A2780 and OVCAR-3 ovarian tumor cells and BJ normal cells, respectively. In each line, from left to right: cells treated with red fluorescent dyes **MBA 2, 3** and **4**. The cell nuclei were counterstained with the blue fluorescent dye DAPI. Scale bar: 20 μm .

In addition to their ability to selectively stain the analysed tumor OVCAR-3, A2780 and healthy BJ ovarian cells, the piperidinyl-carbinol MB analogues **MBA 2-3** exhibited in

vitro cell growth inhibition and influenced the cells metabolic activity. **MBA 2** gave the best biologic outcome, displaying cytotoxicity, cellular, accumulation and multitarget influence on chemoresistant, highly malignant ovarian cells functions, modulating three important molecules with role in cancer cells growth and migration: FOLR1, ICAM-1 and VCAM-1. By functionalization or incorporation into vectors such nanostructures, **MBA 2** has good perspectives to become a promising theragnostic agent.

3.2. New photosensitizers for anticancer photodynamic therapy: efficacy and oxidative stress evaluation in B16F10 melanoma cells

The singlet oxygen generation quantum yields of the studied Methylene Blue analogues **MBA 5-7** were at higher values for compound **5** ($\phi\Delta^1\text{O}_2 = 68\%$) and **6** ($\phi\Delta^1\text{O}_2 = 78\%$) or at least equal (for dye **7** $\phi\Delta^1\text{O}_2 = 52\%$) to that of the standard of the class, MB.

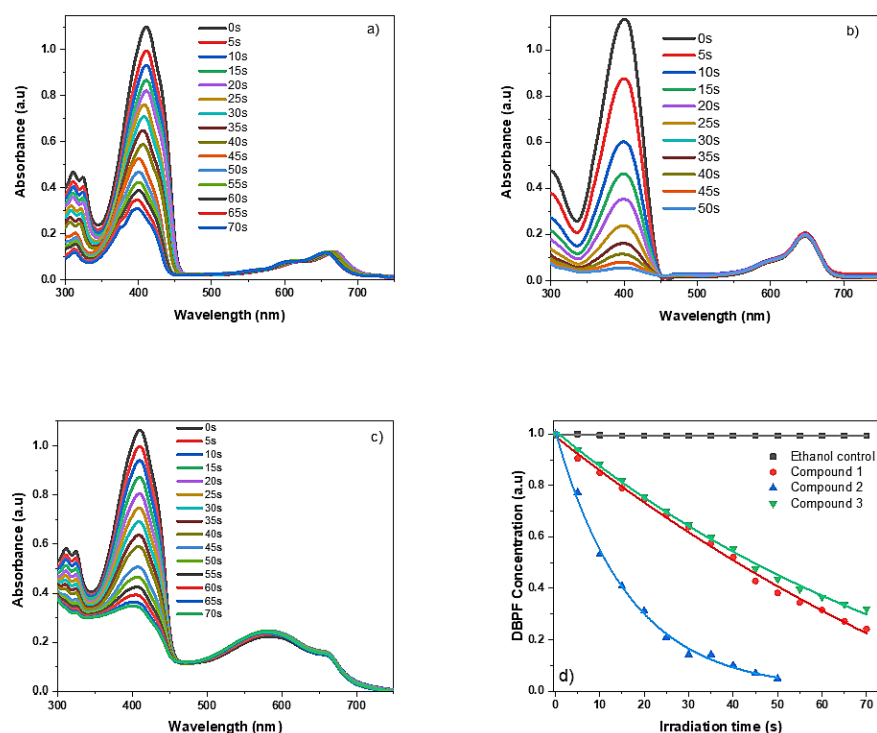


Figure 5. UV-vis spectra of 1,3-diphenylisobenzofuran (DPBF) sensor during irradiation of: a) dye **5** ($C_M = 10^{-6}$ M), b) dye **6** ($C_M = 10^{-6}$ M), c) dye **7** ($C_M = 10^{-5}$ M) ethanolic solution, irradiated with a 660 nm light-emitting-diode (LED) and d) normalized spectra of DPBF degradation in the presence of novel photosensitizers **MBA 5-7**.

The quantum yields for singlet oxygen generation of **MBA 5-7** were calculated from the absorption spectra values of DPBF in the presence of novel dyes **MBA 5-7**, used as

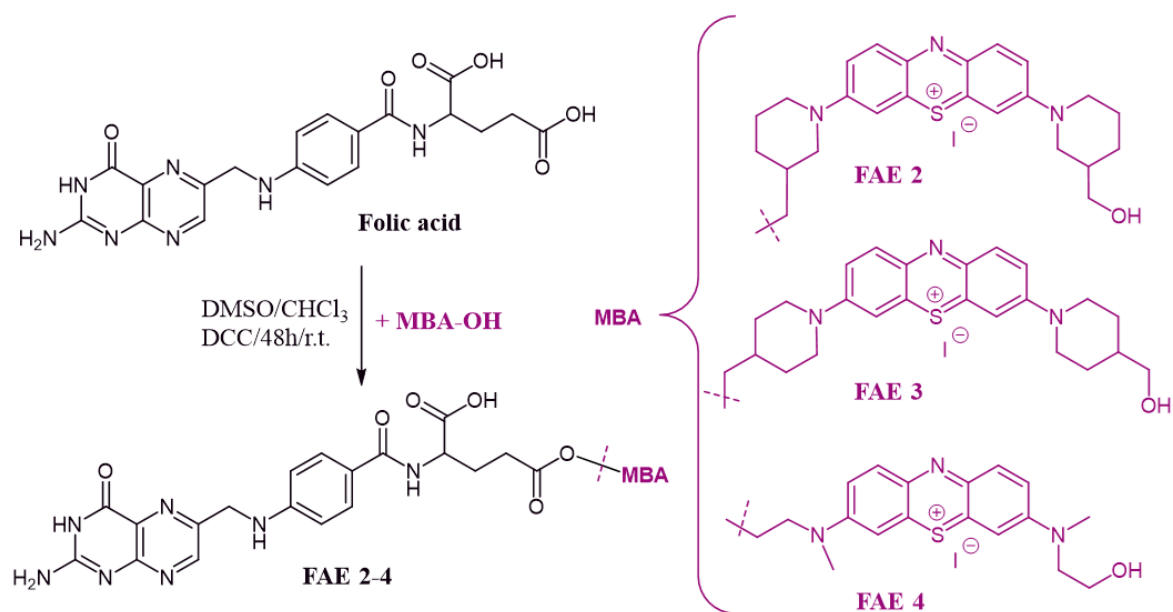
photosensitizers (PS) (Figure 5). **MBA 6**, with the minimal structural complexity, gave the highest quantum yield of singlet oxygen generation value ($\phi\Delta^1\text{O}_2 = 78\%$), the sensor consumption occurring during 50 seconds of irradiation of PS **MBA 6**, compared to PS **MBA 5** and **MBA 7**, which required additional 20 seconds of exposure to 660 nm LED (Figure 5-d)) until the DPBF was completely consumed.

Biological evaluation demonstrated the efficacy of **MBA 5** as a potential candidate for anticancer photodynamic therapy, exhibiting low IC_{50} values and high glutathione reductase activity in both non-irradiated and irradiated cells. **MBA 6** and **MBA 7** showed significant increases in superoxide dismutase activity, with **MBA 5** exhibiting an inhibitory effect on this enzyme.

4. Functionalization of phenothiazinium dyes with folic acid

4.1. Synthesis and structural characterization of the new derivatives

The synthesis of the novel folate derivatives of **MBA 2-4** is illustrated in Scheme 2. Good reaction yields (40-60%) were obtained in the presence of the coupling agent *N,N*-dicyclohexylcarbodiimide (DCC) and catalytic amounts of 4-dimethylaminopyridine (DMAP) in organic solvents (DMSO and chloroform).



Scheme 2. Synthesis of folates **FAE 2-4**.

The formation of the symmetrical 3,7-disubstituted phenazathionium salts **MBA 2-4** and their monoesters with folic acid **FAE 2-4**, as the major reaction product was demonstrated by structural assignments based on mass spectrometry, MALDI-TOF and NMR spectroscopy.

The very low solubility of the new folic acid esters **FAE 2-4**, correlated with their structural complexity brought by lactam/lactim tautomers of the pterin fragment, diastereotopic protons in glutamic acid residues of the folic acid unit, and comparable shielding effects generating accidental isochronism of signals belonging to the folic ester and methylene blue analogues (phenazathionium unit and axial/equatorial protons of piperidiny fragment), make NMR spectra less well resolved. In the ¹H-NMR of **FAE 2-4**, the most deshielded proton in the aromatic region belongs to pterin core and shows the same chemical shift as in the parent folic

acid 8.65 ppm. The signals of the 4-aminobenzoyl unit protons, as well as the methylene or methine protons show similar chemical shifts in **FAE 2-4** as in the folic acid (Figure 6), similar results being already reported^{9,10}.

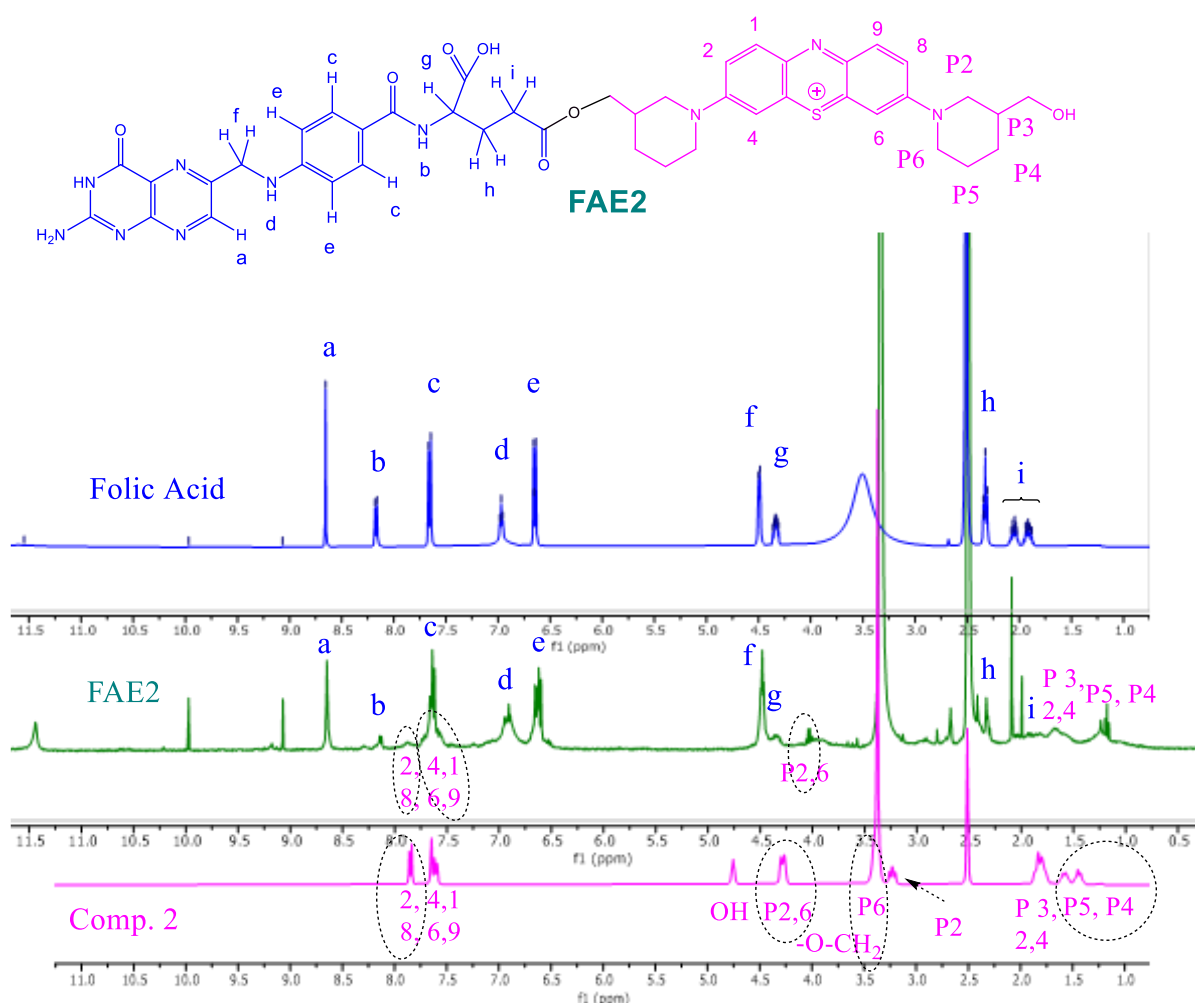


Figure 6. The superimposed 400 MHz ¹H NMR spectra of folic acid (blue), folic ester FAE 2 (green) and compound 2 (magenta).

4.2. Optical and physical properties of the new folates

UV-vis absorption/fluorescence emission spectroscopy was used for investigating the optical properties of the novel **FAE 2-4**. A comparison of the absorption/emission maxima of the folic esters with the parent **MBA 2-4** is presented in Table 2. The **FAE 2-4** exhibited longest wavelength absorption maxima situated in the visible region at similar wavelength positions as **MBA 2-4** parent dyes, typical for the well-known π - π^* electronic transitions of the phenothiazinium chromophore⁴.

Table 2. UV-vis absorption and emission data of **MBA 2-4** and **FAE 2-4** in solution DMSO.

Compd.	$\lambda_{\max\text{abs}}$ [nm]	ϵ [M ⁻¹ cm ⁻¹]	$\lambda_{\max\text{em}}$ [nm]	Fluorescence quantum yield ϕF [%]	Stokes shift [cm ⁻¹]
MBA 2	674 ⁴	5.16x10 ⁴ ⁴	725 ⁴	4.6 ⁴	1043
MBA 3	673 ⁴	3.92x10 ⁴ ⁴	698 ⁴	2.7 ⁴	532
MBA 4	674 ⁴	13.23x10 ⁴ ⁴	697 ⁴	11.1 ⁴	489
FAE 2	680	2.60x10 ³	702; 761	7.5	1565
FAE 3	676	1.27x10 ³	698	5.4	466
FAE 4	669	5.78x10 ³	697	11.2	600

In terms of fluorescence emission, esterification of folic acid with Methylene Blue analogues did not induce a fluorescence quenching, a phenomenon largely encountered when chemically binding to a bulky molecule. In the case of **FAE 3** and **FAE 4** folates, no shift of the emission maximum is observed: the fluorescence emission wavelength remains at the same values as the free analogues **MBA 3** ($\lambda_{\max} = 698$ nm) and **MBA 4** ($\lambda_{\max} = 697$ nm). For **MBA 2**, binding to folic acid resulted in a bathochromic shift of the emission maximum from 725 nm in **MBA 2** to 761 nm in **FAE 2**, according to the second emission maximum. The fluorescence emission quantum yields of folate esters in DMSO show the highest $\phi\text{F} = 11.2\%$ for **FAE 4** similar with its **MBA 4**, and the $\phi\text{F} = 7.5\%$ for **FAE 2** and $\phi\text{F} = 5.4\%$ for **FAE 3** being higher than their precursor **MBA 2** and **MBA 3**.

4.3. New photosensitizers for antimicrobial photodynamic therapy: efficacy evaluation on Gram-positive and Gram-negative bacterial strains

All Methylene Blue analogues and their folates were able to generate singlet oxygen close to the yield generated by the parent compound ($\phi\Delta^1\text{O}_{2\text{MB}} = 52\%$)¹¹; however this finding alone does not necessarily indicate activity against target cells, because this is reliant on the ultimate cellular environment, and the PS ability to penetrate and accumulate in the target cells and under light irradiation to induce the formation of singlet oxygen¹².

From the absorption spectra of DPBF in the presence of **MBA 2-4** or **FAE 2-4** as photosensitizers, the singlet oxygen quantum yields were calculated. The best results were

show by **MBA 4**, which exhibits a singlet oxygen generation quantum yield value of 61%. The folic esters reveal a significant decrease in singlet oxygen quantum yields compared to their **MBA** precursors ($\phi\Delta^1\text{O}_2$: 19% **FAE 2**/ 47% **MBA 2**, 12% **FAE 3**/ 59% **MBA 3**, 28% **FAE 2** /61%, **MBA 4**).

The minimum inhibitory concentration was evaluated for the synthesized compounds in comparison with the standard class - parent compound (Methylene Blue), both with and without LED irradiation for photodynamic therapy. Our findings reveal significant improvements in antimicrobial activity for the synthesized compounds, especially when coupled with PDT.

Across all comparisons, the six synthesized compounds consistently demonstrated superior antimicrobial activity compared to the standard Methylene Blue, for example the MIC for *Deinococcus radiodurans* is 400 μM for MB while MBA are far more efficient – with 29 μM for **MBA 2-3** and 134 μM for **MBA 4** without irradiation; this trend is evident in both PDT and non-PDT conditions. The binding of folic acid moieties to the **MB** analogues further enhanced their antimicrobial potential.

Remarkably, irradiation with a 660 nm LED significantly augmented the antimicrobial efficacy of all compounds. This effect can be attributed to the generation of reactive oxygen species (ROS) during photodynamic therapy, which enhances the compounds' antimicrobial activity by causing oxidative damage to microbial cells. The ROS-mediated mechanism amplifies the compounds' bactericidal effects, leading to a notable reduction in MIC values. In this case for all compounds there is an approximately fourfold decrease in MIC values.

5. Transient radical species of phenothiazinium dyes and oxygen indicators

In this study ¹³, Methylene Blue and methylene blue analogues **MBA 2-4** were investigated as possible oxygen indicators turning blue at low levels of oxygen in the atmosphere. This study features the mechanistic aspects of the redox process involving MB and its analogues, using electron paramagnetic resonance (EPR) and UV-vis spectroscopy. Based on EPR spectroscopy, the presence of the MB radical species generated in the redox process, in the presence of the reducing agent-glucose in KOH medium, has been highlighted. Based on EPR measurements, we demonstrated that the free electron is located to the nitrogen atom of the phenothiazine core, both in the case of **MB** and its three studied analogues.

All the tested compounds gave promising results in the preparation of two types of oxygen indicators suitable for packaging applications: a) photochemical indicator using phenothiazinium dyes deposited on a polyvinyl alcohol support together with TiO₂ photocatalyst, and b) chemical indicator using a mixture of phenothiazin-5-ium dye, glucose, and KOH incorporated in a carboxymethylcellulose polymer matrix. All sensors proved to be very sensitive, with the colour change occurring at volumetric concentrations below 0.01% O₂ in the vacuumed package atmosphere.

5.1. UV-vis experiments documentation of transient radical species

The optical properties of the leuco-forms of **MB** and **MBA 2-4**, and their colour change during the oxidation process was investigated by UV-vis spectroscopy. Leuco-forms of MB and **MBA 2-4** were generated *in situ* from a mixture of the corresponding dye with the reducing agent under argon atmosphere and their UV-vis spectra were further recorded. In all cases the wavelength around 259 nm characteristic for phenothiazine chromophore ¹⁴ were identified in UV region, cf. Table 3.

During the oxidation process of the leuco-forms of MB and **MBA 2-4**, their UV-vis spectrum appears modified by the appearance of a transient absorption maximum situated in the region 552-592nm, (Table 3). These absorption maxima are reminiscent of those previously assigned to a transient aminyl radical species generated in the oxidation process of phenothiazines ¹⁵. These species were therefore further investigated by EPR spectroscopy.

Table 3. Characteristic UV-vis wavelength absorbance maxima of MB and **MBA 2-4** derivatives, containing 0.1M KOH(aq): 1M Glucose(aq):1M phenothiazin-5-ium dye (ethanol solution) (v/v/v 1/1/1).

Phenothiazinium dye	$\lambda_{\text{max,abs}}$ [nm]		
	Oxidized form	Free radical	Leuco-form
1 (MB)	612; 664	552	311; 252
MBA 2	628; 678	592	296; 259
MBA 3	620; 674	588	315; 255
MBA 4	614; 662	591	318; 257

5.2. Electron paramagnetic resonance experiments

The free radical intermediates of all four compounds yielded almost indistinguishable isotropic EPR spectra easily recognisable as a nitrogen-centred free radical with triplet hyperfine splitting, which arises due to the coupling between the magnetic moment of the unpaired electron ($S=1/2$) with the magnetic moment of the ^{14}N nucleus ($I=1$). The similarity between the four compounds is in line with the assignment of the radical as centred on the core of the heterocyclic unit and with little perturbation from the substituents at the tertiary amine groups.

5.3. Oxygen colorimetric indicators

Two types of oxygen optical sensors have been successfully formulated by using phenothiazinium dyes (**MB** and analogues **MBA 2-4**) incorporated into an oxygen permeable polymeric matrix such as carboxymethyl cellulose (ChOxIn) or polyvinyl alcohol (PhOxIn). In reducing media, the colourless leuco form of the dye is perceivable, followed by colour turn to blue upon oxidation. Both indicators can be easily activated in vacuum in the presence of glucose as chemical reducing agent (ChOxIn) or TiO_2 photochemical reducing agent and UV light irradiation ($\lambda=250$ nm) (PhOxIn).



Figure 7. The reversible chromogenic process for photochemical Oxygen-indicators containing titanium dioxide, glycerol, polyvinyl alcohol and phenothiazinium dye: a) **MB**, b) **MBA 2**.

6. Conclusions

Seven compounds from the class of phenothiazinium salts, analogues of methylene blue, were synthesized. The synthesis of all the compounds was accomplished both by the classical synthetic procedure and by other three more environmentally friendly methods, namely, ultrasound assisted synthesis (direct and indirect irradiation) and mechanochemical procedure. The phenothiazinium dyes **MBA 2-4** were functionalized by esterification reaction with folic acid. Structural assignments based on high resolution mass spectrometry (HRMS) and NMR spectroscopy confirmed the formation of the symmetrical 3,7-disubstituted phenothiazinium salts **MBA 2-7** and the **FAE 2-4** folates as the main reaction product. For **MBA 6**, crystals suitable for single crystal X-ray diffraction were obtained and the XRD was recorded.

Using UV-vis absorption and fluorescence emission spectroscopy, the photophysical properties of the new phenothiazinium dyes were evaluated and compared with the parent MB. The visible absorption maxima wavelength for **MBA** novel compounds in ethanolic solution are in the 555-668 nm range. When **MBA 2-6** were excited by the longest wavelength absorption maxima, the novel compounds dissolved in ethanol emitted fluorescence with maximum intensity in the visible range (670-715 nm). **MBA 2** and **MBA 4**, gave the higher fluorescence quantum yield, 4.6% for **MBA 2** and 11.1% for **MBA 4**.

The **FAE 2-4** exhibited longest wavelength absorption/emission maxima situated in the visible region at similar wavelength positions as **MBA 2-4** parent dyes. The covalent binding of **MBA 2-4** ($\lambda_{\text{abs,max}} \sim 674$ nm) to folic acid ($\lambda_{\text{abs,max}} \sim 285$ nm) did not produce a significant shift of the FAE absorption maxima because the aliphatic bridges separating the phenothiazinium chromophore from the aromatic components of folic acid restrict the extension of the π electron conjugation. The fluorescence emission quantum yields of folate esters in DMSO show the highest $\Phi_F = 11.2\%$ for **FAE 4** similar with its **MBA 4**, and the $\Phi_F = 7.5\%$ for **FAE 2** and $\Phi_F = 5.4\%$ for **FAE 3** being higher than their precursor **MBA 2** and **MBA 3**.

The partition coefficient of the dyes **MBA 2-7** was estimated in an *n*-octanol/water system, revealing a hydrophilic character comparable to **MB** for **MBA 2, 3** and a higher hydrophilicity for the **MBA 4-6** dyes. In contrast, **MBA 7** is undoubtedly a lipophilic compound, due to its 4-phenyldiazenylaniline aromatic auxochrome substituents.

The compatibility of **MBA 2-4** with the biological environment, assumed at the design stage by selecting as auxochrome of the phenothiazinium chromophore the bulky heterocyclic piperidine decorated with hydrophilic functionalities for compounds **MBA 2** and **3**, was supported by experimental results. In addition to their ability to selectively stain the analysed tumor OVCAR-3, A2780 and healthy BJ ovarian cells, the piperidinyl-carbinol phenothiazinium dyes **MBA 2** and **3** exhibited *in vitro* cell growth inhibition and influenced the cells metabolic activity. **MBA 2** gave the best biologic outcome, displaying cytotoxicity, cellular, accumulation and multitarget influence on chemo-resistant, highly malignant ovarian cells functions.

The second biological activity study involved **MBA 5-7** testing as photosensitisers for the treatment of B16F10 melanoma cells. The singlet oxygen generation quantum yields of the new dyes were at higher values for **MBA 5** ($\phi\Delta^1\text{O}_2 = 68\%$) and **MBA 6** ($\phi\Delta^1\text{O}_2 = 78\%$) or at least equal (for dye **MBA 7** $\phi\Delta^1\text{O}_2 = 52\%$) to that of the standard of the class, MB. Biological evaluation demonstrated the efficacy of **MBA 5** as a potential candidate for anticancer photodynamic therapy, exhibiting low IC_{50} values and high glutathione reductase activity in both non-irradiated and irradiated cells.

The folic acid esters were tested as photosensitizers for antimicrobial photodynamic therapy. Their efficacy evaluation was made on Gram-positive and Gram-negative bacterial strains. The binding of folic acid to the **MBA** offered the possibility of targeting the folic acid metabolism pathway of microbial cells and/or more efficiently adhere to the lipid bilayer of the membranes, without compromising the photosensitizer's optical properties. **FAE** demonstrated enhanced potency, targeting specificity, and notably lower minimum inhibitory concentrations (MIC) values, indicating their potential as highly effective antimicrobial agents.

MB and the methylene blue analogues **MBA 2-4** were also investigated as possible oxygen indicators turning blue at low levels of oxygen in the atmosphere. This study also included mechanistic aspects of the redox process involving MB and its analogues, using electron paramagnetic resonance (EPR) and UV-vis spectroscopy. Using EPR spectroscopy, the generation of radical species on MB and on its derivatives/analogues by the reducing agent (glucose in alkaline medium), was confirmed. The free electron displayed hyperfine interaction with nitrogen atom of the phenothiazine core in all cases. The radical species of the four tested compounds, MB and **MBA 2-4** were also observable in UV-vis experiments, with characteristic maxima at 552–592 nm. All the tested compounds gave promising results in the preparation of two types of oxygen indicators suitable for packaging applications: a) photochemical indicator

using phenothiazinium dyes deposited on a polyvinyl alcohol support together with TiO₂ photocatalyst, and b) chemical indicator using a mixture of phenothiazinium dye, glucose, and KOH incorporated in a carboxymethylcellulose polymer matrix. All sensors proved to be very sensitive, with the colour change occurring at volumetric concentrations below 0.01% O₂ in the vacuumed package atmosphere.

References

- (1) Gopi, C.; Dhanaraju, M. D. Recent Progress in Synthesis, Structure and Biological Activities of Phenothiazine Derivatives. *Rev. J. Chem.* **2019**, *9* (2), 95–126. <https://doi.org/10.1134/s2079978019020018>.
- (2) Padnya, P. L.; Khadieva, A. I.; Stoikov, I. I. Current Achievements and Perspectives in Synthesis and Applications of 3,7-Disubstituted Phenothiazines as Methylene Blue Analogues. *Dye. Pigment.* **2023**, *208*, 110806. <https://doi.org/10.1016/j.dyepig.2022.110806>.
- (3) Thesnaar, L.; Bezuidenhout, J. J.; Petzer, A.; Petzer, J. P.; Cloete, T. T. Methylene Blue Analogues: In Vitro Antimicrobial Minimum Inhibitory Concentrations and in Silico Pharmacophore Modelling. *Eur. J. Pharm. Sci.* **2021**, *157* (October 2020), 105603. <https://doi.org/10.1016/j.ejps.2020.105603>.
- (4) Stoean, B.; Gaina, L.; Cristea, C.; Silaghi-Dumitrescu, R.; Branzanic, A. M. V.; Focsan, M.; Fischer-Fodor, E.; Tigiu, B.; Moldovan, C.; Cekan, A. D.; Achimas-Cadariu, P.; Astilean, S.; Silaghi-Dumitrescu, L. New Methylene Blue Analogues with N-Piperidinyl-Carbinol Units: Synthesis, Optical Properties and in Vitro Internalization in Human Ovarian Cancer Cells. *Dye. Pigment.* **2022**, *205*, 110460. <https://doi.org/10.1016/J.DYEPIG.2022.110460>.
- (5) Stoean, B.; Lupan, I.; Cristea, C.; Sillion, M.; Silaghi-Dumitrescu, L.; Silaghi-Dumitrescu, R.; Gaina, L. Outcomes of Folic Acid Esterification upon the Properties of Hydrophilic Phenothiazinium Dyes: New Photosensitizers for Antimicrobial Photodynamic Therapy. *J. Photochem. Photobiol. A Chem.* **2024**, 115500. <https://doi.org/10.1016/J.JPHOTOCHEM.2024.115500>.
- (6) Xiao, Q.; Lin, H.; Wu, J.; Pang, X.; Zhou, Q.; Jiang, Y.; Wang, P.; Leung, W.; Lee, H.; Jiang, S.; Yao, S. Q.; Gao, L.; Liu, G.; Xu, C. Pyridine-Embedded Phenothiazinium Dyes as Lysosome-Targeted Photosensitizers for Highly Efficient Photodynamic Antitumor Therapy. *J. Med. Chem.* **2020**, *63* (9), 4896–4907. <https://doi.org/10.1021/acs.jmedchem.0c00280>.
- (7) Gorman, S. A.; Bell, A. L.; Griffiths, J.; Roberts, D.; Brown, S. B. The Synthesis and Properties of Unsymmetrical 3,7-Diaminophenothiazin-5-Ium Iodide Salts: Potential

- Photosensitisers for Photodynamic Therapy. *Dye. Pigment.* **2006**, *71* (2), 153–160. <https://doi.org/10.1016/j.dyepig.2005.06.011>.
- (8) Gollmer, A.; Felgenträger, A.; Bäumlner, W.; Maisch, T.; Späth, A. A Novel Set of Symmetric Methylene Blue Derivatives Exhibits Effective Bacteria Photokilling - A Structure-Response Study. *Photochem. Photobiol. Sci.* **2015**, *14* (2), 335–351. <https://doi.org/10.1039/c4pp00309h>.
- (9) Yallappa, S.; Manjanna, J.; Dhananjaya, B. L.; Vishwanatha, U.; Ravishankar, B.; Gururaj, H. Phytosynthesis of Gold Nanoparticles Using Mappia Foetida Leaves Extract and Their Conjugation with Folic Acid for Delivery of Doxorubicin to Cancer Cells. *J. Mater. Sci. Mater. Med.* **2015**, *26* (9), 1–12. <https://doi.org/10.1007/s10856-015-5567-3>.
- (10) Gocheva, G.; Petkov, N.; Garcia Luri, A.; Iliev, S.; Ivanova, N.; Petrova, J.; Mitrev, Y.; Madjarova, G.; Ivanova, A. Tautomerism in Folic Acid: Combined Molecular Modelling and NMR Study. *J. Mol. Liq.* **2019**, *292*, 111392. <https://doi.org/10.1016/j.molliq.2019.111392>.
- (11) Korínek, M.; Dědic, R.; Molnár, A.; Svoboda, A.; Hála, J. A Comparison of Photosensitizing Properties of Meso-Tetraphenylporphin in Acetone and in Dimethyl Sulfoxide. *J. Mol. Struct.* **2005**, *744–747* (SPEC. ISS.), 727–731. <https://doi.org/10.1016/j.molstruc.2004.11.036>.
- (12) Wainwright, M.; Meegan, K.; Loughran, C.; Giddens, R. M. Phenothiazinium Photosensitisers, Part VI: Photobactericidal Asymmetric Derivatives. *Dye. Pigment.* **2009**, *82* (3), 387–391. <https://doi.org/10.1016/j.dyepig.2009.02.011>.
- (13) Stoean, B.; Lehene, M.; Zagrean-Tuza, C.; Silaghi-Dumitrescu, R.; Cristea, C.; Gaina, L. Transient Radical Species and Oxygen Colorimetric Indicators Grounded on Phenothiazinium Dyes. *Spectrochim. Acta Part A Mol. Biomol. Spectrosc.* **2024**, *320*, 124602. <https://doi.org/10.1016/J.SAA.2024.124602>.
- (14) Molnar, E.; Gal, E.; Gaina, L.; Cristea, C.; Fischer-Fodor, E.; Perde-Schrepler, M.; Achimas-Cadariu, P.; Focsan, M.; Silaghi-Dumitrescu, L. Novel Phenothiazine-Bridged Porphyrin-(Hetero)Aryl Dyads: Synthesis, Optical Properties, in Vitro Cytotoxicity and Staining of Human Ovarian Tumor Cell Lines. *Int. J. Mol. Sci.* **2020**, *21* (9), 3178. <https://doi.org/10.3390/ijms21093178>.

- (15) Bodea Cornel; Silberg, I. A. Octachlorophenothiazinyl: A Very Stable Nitrogen Radical.
Nature **1963**, *198* (4003), 883–884. <https://doi.org/https://doi.org/10.1038/198883a0>.

